PAPER • OPEN ACCESS

Dark state, zero-index and topology in phononic metamaterials with negative mass and negative coupling

New Journal of Physics
The open access journal at the forefront of physics

Deutsche Physikalische Gesellschaft DPG
IOP Institute of Physics

Published in partnership with: Deutsche Physikalische Gesellschaft and the Institute of Physics

OPEN ACCESS

RECEIVED
25 April 2019

REVISED
30 July 2019

ACCEPTED FOR PUBLICATION
29 August 2019

PUBLISHED
17 September 2019

PAPER

Dark state, zero-index and topology in phononic metamaterials with negative mass and negative coupling

Danmei Zhang[1], **Jie Ren**[1,3], **Tianxiong Zhou**[1] **and Baowen Li**[2]

[1] Center for Phononics and Thermal Energy Science, China-EU Joint Center for Nanophononics, Shanghai Key Laboratory of Special Artificial Microstructure Materials and Technology, School of Physics Sciences and Engineering, Tongji University, Shanghai 200092, People's Republic of China
[2] Department of Mechanical Engineering, University of Colorado Boulder, CO 80309 United States of America
[3] Author to whom any correspondence should be addressed.

E-mail: Xonics@tongji.edu.cn

Keywords: zero-index, topology, phononic metamaterial, double negative, dark state

Abstract

Phononic metamaterials have attracted extensive attention since they are flexibly adjustable to control the transmission. Here we study a one-dimensional phononic metamaterial with negative mass and negative coupling, made of resonant oscillators and chiral couplings. At the frequency where the effective mass and coupling are both infinite, a flat band emerges that induces a sharply high density of states, reminiscent of the phononic dark states. At the critical point of band degeneracy, a phononic Dirac-like point emerges where both the effective mass and the inverse of effective coupling are simultaneously zero, so that zero-index is realized for phonons. Moreover, the phononic topological phase transition is observed when the phononic band gap switches between single mass-negative and single coupling-negative regimes. When these two distinct single negative phononic metamaterials are connected to each other, a phononic topological interface state is identified within the gap, manifested as the phononic counterpart of the topological Jackiw–Rebbi solution.

1. Introduction

Metamaterials usually exhibit extraordinary properties that can not found in nature like the negative permittivity (ε), negative magnetic permeability (μ) of electromagnetical metamaterials which can realize reversed Doppler effect, reversed Cherenkov radiation and negative refraction index [1–6]. Along with the electromagnetical metamaterials for photonics, the phononic metamaterials have been greatly developed in recent years. In 2000, the phononic crystal with local resonance is proposed and the effective negative parameter is introduced [7]. Then a variety of metamaterials comprising solid and liquid are proved to have double negative properties [8–12] which are reminiscent of Mie resonance. With the development of the theory, the negative modulus is demonstrated [13] by the array of subwavelength Helmholtz resonators or side holes on a tube [14] and the negative mass is realized by membrane-type acoustic tube [15] in low frequency range. After, the double negative parameters in the structure with array of periodic thin membranes and side holes [16] are proposed. Then, non-periodic space-coiling structures [17, 18] with double negativity are demonstrated to exhibit negative refractive index. In addition to the Mie resonance mechanism, there are also multiple scattering mechanisms leading to negative effective parameters [19, 20].

The mass-spring structure with different coupling and spatial distribution can also have negative effective parameters [21–27] because of Bragg scattering and resonant mechanism in different frequency regimes. In 2007, following the work of [7], Milton and Willis proposed a mass-in-mass system and showed that the dynamic effective mass of composite materials, defined in the framework of Newton's law of motion (contrary to the static gravitational mass), exhibits the existence of single or double negative properties [23]. In 2008, Yao *et al* experimentally examined the model of mass-spring systems [24] with effective negative mass. Additionally in 2011, Liu *et al* proposed an elastic model with double negative parameters by integrating a tri-chiral lattice

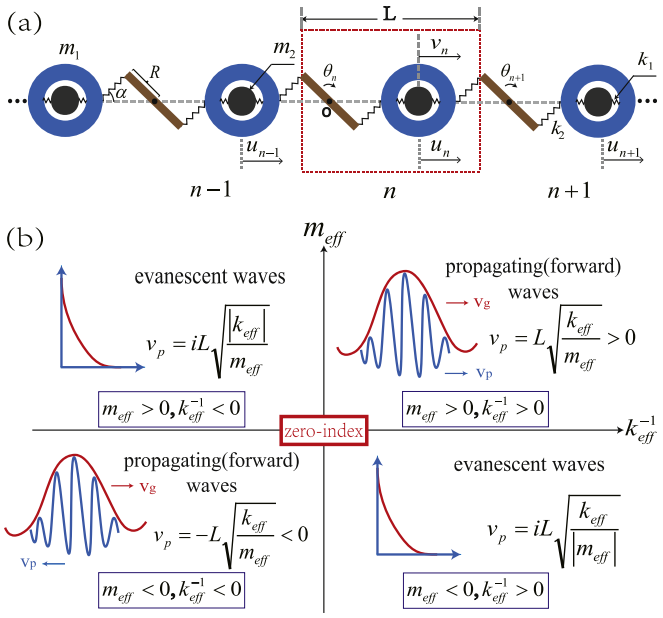

Figure 1. (a) The one-dimension chiral lattice model with both negative mass and negative coupling. (b) Classification of materials according to effective mass m_{eff} and inverse of effective spring coupling k_{eff}^{-1}. v_p is the phase velocity and v_g is the group velocity.

with softly coated inclusions [25] and an other double negative systems constructed by chiral mass-spring unit [26]. Since then, a plenty of phononic metamaterials based on chiral and spiral structures are proposed [28–30].

On the other hand, there are many other properties of phononic metamaterials attracting increasing interest recent years, such as the zero refraction index (zero-index for short) and topological bands. In zero-index metamaterials, waves does not carry any spatial phase changes and the wave length is effectively infinite long [31] which can be used in wave surface modulation and bending waveguides. The zero-index material has been proved experimentally in the electromagnetic wave [32, 33] and the acoustic and phononic counterparts have also been discussed [34–38]. Meanwhile, over the past decades, the concept of 'topology' has been attracting extensive research interests in phononics and phononic metamaterials [39–44]. Many interesting topological phenomena, such as topological interface and edge states [45–47], have been observed in phononic metamatericals.

In this work, we study a 1D phononic metamaterials of mechanical resonant oscillators and chiral couplings. We analyze the phononic band structure by diagonalizing the dynamic matrix, calculate the effective mass and effective coupling by the equation of motion, and study the corresponding transmittance with transfer matrix method. We show that by design, the oscillator mass and inter-oscillator coupling, although both are positive naturally, can be either single negative or double negative effectively within a certain frequency range. At the frequency where the effective mass and coupling are both infinite, a flat band emerges that will induce a sharply high density of states, reminiscent of the phononic dark states. Moreover, a Dirac-like point of phononic band emerges when both effective mass and the inverse of effective coupling are simultaneously zero, so that zero-index is realized for phonons. Finally, we report the phononic topological phase transition that the phononic band gap switches between single mass-negative and single coupling-negative regime. Accordingly, a topological interface state is identified between two different single negative phononic materials.

2. Model and method

The system with resonant mass [23] and chiral spring coupling [26, 25] is shown in figure 1(a). The mass-in-mass unit takes the form of a rigid ball with mass m_1 and contains an internal mass m_2 that is connected to the outer ball by two internal spring k_1. In addition, we add a rigid leverage as the inter-unit coupling, whose moment of inertia and radius are J and R. The middle of the leverage is fixed at the point O and both ends are connected to the outer balls by the spring k_2. α is the equilibrium angle between k_2 and horizontal axis. The lattice constant of the system is L. For m_1 and m_2, only the movements in the horizontal direction x are considered for simplicity.

Similar to photonic metamaterials, the phononic metamaterials can be generally classified into four different categories according to the effective inverse coupling and mass (k_{eff}^{-1}, m_{eff}) shown in figure 1(b). When they are double positive, the phase velocity is a positive number. The direction of phase velocity and group velocity are

the same and the wave can propagate forward just like in the natural materials with normal refraction. But when one of $(k_{\text{eff}}^{-1}, m_{\text{eff}})$ is negative, we can see that the phase velocity is an imaginary number. According to the harmonic wave solution, the wave will present an evanescent wave of exponential decay. The third quadrant is when $(k_{\text{eff}}^{-1}, m_{\text{eff}})$ are both negative. In this case, the direction of phase velocity and group velocity is sign opposite and the wave can still propagate but with anomalous negative refraction. At the origin of the axes, the material possesses zero-index where the effective mass and the inverse of effective spring coupling are both zero, i.e. the refractive index equals to zero and the wave can propagate perfectly.

From the Newton's laws, the equations of motion for the nth unit are given by

$$m_1\frac{\mathrm{d}^2u_n}{\mathrm{d}t^2} = -2k_1(u_n - v_n) - k_2(u_n\cos\alpha - \theta_{n+1}R)\cos\alpha - k_2(u_n\cos\alpha + \theta_n R)\cos\alpha, \tag{1}$$

$$m_2\frac{\mathrm{d}^2v_n}{\mathrm{d}t^2} = -2k_1(v_n - u_n), \tag{2}$$

$$J\frac{\mathrm{d}^2\theta_n}{\mathrm{d}t^2} = -k_2(2\theta_n R - u_{n-1}\cos\alpha + u_n\cos\alpha)R, \tag{3}$$

where u_n (v_n) denotes the displacement of mass 1 (2) in the nth cell, θ_n is the angle displacement of the leverage. Under harmonic excitation, as we all know, the harmonic wave solution of the 1D lattice chain is $(u_n, v_n, \theta_n) = (\hat{u}, \hat{v}, \hat{\theta})\mathrm{e}^{\mathrm{i}(-nqL+\omega t)}$, with q the quasi-momentum. So from equations (2) and (3) we can have:

$$v_n = \frac{2k_1u_n}{2k_1 - m_2\omega^2}, \tag{4}$$

$$\theta_n = \frac{k_2R\cos\alpha}{J\omega^2 - 2k_2R^2}(u_n - u_{n-1}). \tag{5}$$

By substituting these equations into equation (1), we can reorganize the equation and obtain the following result:

$$-m_{\text{eff}}\omega^2u_n = -k_{\text{eff}}(2u_n - u_{n+1} - u_{n-1}), \tag{6}$$

where

$$m_{\text{eff}} = m_1 - \frac{2k_1}{\omega^2} + \frac{4k_1^2}{(2k_1 - m_2\omega^2)\omega^2} - \frac{2k_2\cos^2\alpha}{\omega^2},$$
$$k_{\text{eff}} = \frac{k_2^2R^2\cos^2\alpha}{J\omega^2 - 2k_2R^2}. \tag{7}$$

The m_{eff} and k_{eff} are the effective atomic mass and effective inter-atomic coupling of the system, which is equivalent to a 1D monatomic chain. As we can see that the effective coupling is only related to the rotational vibration resonance; the effective mass is not only related to the rotational vibration resonance but also related to the translational vibration resonance of the outer-inter masses. Therefore, the dispersion relationship can be obtained by the effective parameters:

$$\omega^2 = 4\frac{k_{\text{eff}}}{m_{\text{eff}}}\sin^2\frac{qL}{2}. \tag{8}$$

Note since k_{eff} and m_{eff} are both functions of ω^2, the band will split into three branches as we will see in the following.

Alternatively, by letting the determinant of the system's dynamic matrix equal to zero:

$$\mathrm{Det}\begin{pmatrix} 2k_2\cos^2\alpha + 2k_1 - m_1\omega^2 & -2k_1 & k_2R\cos\alpha(1 - \mathrm{e}^{-\mathrm{i}qL}) \\ -2k_1 & 2k_1 - m_2\omega^2 & 0 \\ k_2R\cos\alpha(1 - \mathrm{e}^{\mathrm{i}qL}) & 0 & 2k_2R^2 - J\omega^2 \end{pmatrix} = 0, \tag{9}$$

we can also get the dispersion relation $\omega(q)$ (frequency $f = \omega/2\pi$) of this model, as exemplified in figure 2(a). Because each unit cell has three degrees of freedom, there are three pass bands in the simplest Brillouin zone (the same result of the dispersion relation is obtained if using formula equation (8)). We can see that the slope of the upper band is positive. So the direction of the group velocity and phase velocity are the same, which means that in this frequent range, the material has both positive mass and couplings, corresponding to the first quartile of figure 1(b). However, the slope of the middle band and lower band are negative with positive phase velocity, which means that the group velocity is also negative and corresponds to the negative refraction in the third quartile of figure 1(b).

But, for the two forbidden band gaps, we are not sure whether they are caused from translation resonance, rotation resonance or Bragg scattering, and which kinds of single negative are they. In order to further understand the underlying reason, we respectively check the effective mass m_{eff} and the inverse of effective coupling k_{eff}^{-1} versus frequency f, as shown in figures 2(b)–(c) according to equation (7). We can see that the

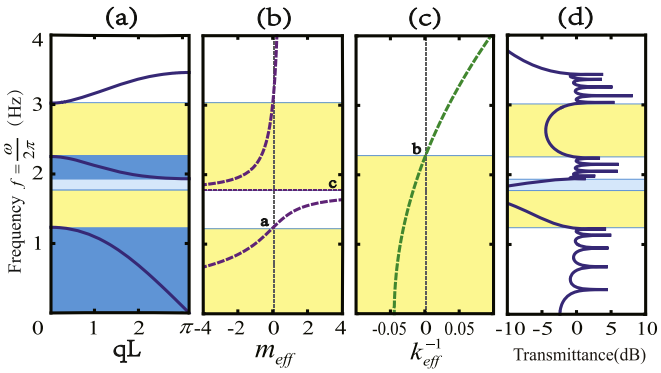

Figure 2. (a) The dispersion relation of the model (frequency $f = \omega/2\pi$). (b) The effective mass m_{eff} versus frequency f. (c) The inverse of effective spring coupling k_{eff}^{-1} versus frequency f. (d) The transmittance spectrum of the system composed of five units ($N = 5$). where $m_1 = 0.5\,\text{kg}$, $m_2 = 0.5\,\text{kg}$, $k_1 = 30\,\text{N m}^{-1}$, $k_2 = 60\,\text{N m}^{-1}$, $J = 0.0015\,\text{kg m}^2$, $R = 0.05\,\text{m}$, $\alpha = \pi/6$. Points a, b and c respectively represents the frequency when $m_{\text{eff}} = 0$, $k_{\text{eff}}^{-1} = 0$ and $m_{\text{eff}} = \infty$. Yellow areas correspond to single negative area and blue areas correspond to double negative area.

middle and bottom bands correspond to both negative mass and negative spring coupling. That is to say, the two lower bands are double negative, agreeing well with our analysis above. It should be noticed that there appears a Bragg scattering induced gap below the bottom of the middle band, although within double negative regime. Besides, as displayed in figures 2(b) and (c), the upper band gap and lower band gap corresponds to the single mass negative and single coupling negative, separately. Therefore the system will exhibit different properties under different frequency ranges.

Besides, we use the transfer matrix method to discuss the phononic transmission properties of the metamaterial. Our structure can be considered as an effective 1D monatomic lattice. Based on the previous calculation method [24], the transmittance of the system is defined as $T = |\prod_{n=1}^{N} T_n|$, $T_n = u_n/u_{n-1}$, N is the number of unit cell. Thus, for the uniform 1D phononic metamaterial with N unit, the recursive relation:

$$(2k_{\text{eff}} - \omega^2 m_{\text{eff}})u_n = k_{\text{eff}}(u_{n+1} + u_{n-1}),\ n = 1, 2, \ldots N-1;\ (k_{\text{eff}} - \omega^2 m_{\text{eff}})u_N = k_{\text{eff}}\,u_{N-1}, \tag{10}$$

leads to the nth transmittance T_n, expressed as:

$$T_n = \frac{k_{\text{eff}}}{k_{\text{eff}}(2 - T_{n+1}) - m_{\text{eff}}\,\omega^2},\ n = 1, 2 \ldots N \tag{11}$$

with $T_{N+1} = 1$.

We plot the transmittance $T = |\prod_{n=1}^{N} T_n|$ of the system (with 5 units, $N = 5$) in figure 2(d). From the colorized area of the figure, we can see that when the driving frequency matches well with the band gap, the system will have strong reflection and the transmittance is very small. The blue area is caused from Bragg scattering although it is in double negative range and yellow areas correspond to the band gap induced by the single negative properties, which means that in the process of wave propagation, the wave present an evanescent wave of exponential decay leading to the vanishing transmittance within a certain frequency range.

3. Results and discussions

3.1. Flat band and dark states

As we can see from figure 2 and following figures 3–5, we mark three points a, b and c of special frequencies in the bands, corresponding to $m_{\text{eff}} = 0$, $k_{\text{eff}}^{-1} = 0$, $m_{\text{eff}} = \infty$, respectively. According to the formula of effective parameters equation (7), the frequency of points a, b and c at long wavelength limit are :

$$f_a = \frac{\omega_a}{2\pi} = \frac{1}{2\pi\sqrt{m_1 m_2}}(k_1(m_1 + m_2) + k_2 m_2 \cos^2\alpha + \sqrt{(k_1(m_1 + m_2) + k_2 m_2 \cos^2\alpha)^2 - 4m_1 m_2 k_1 k_2 \cos^2\alpha}\,)^{\frac{1}{2}}, \tag{12}$$

$$f_b = \frac{\omega_b}{2\pi} = \frac{1}{\pi}\sqrt{\frac{R^2 k_2}{2J}}, \tag{13}$$

$$f_c = \frac{\omega_c}{2\pi} = \frac{1}{\pi}\sqrt{\frac{k_1}{2m_2}}. \tag{14}$$

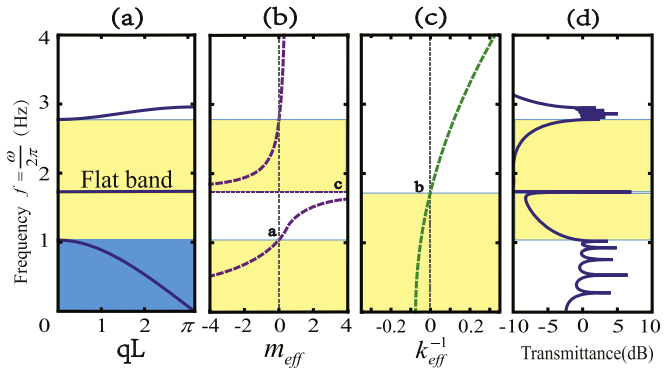

Figure 3. (a) The dispersion relation of the model with a flat band at the condition $f_c = f_b$. (b)–(d) The effective mass, inverse of effective spring coupling and the transmittance spectrum for the system of five units ($N = 5$) with lattice parameters $k_2 = 36$ N m^{-1}. Other parameters are the same as used in figure 2.

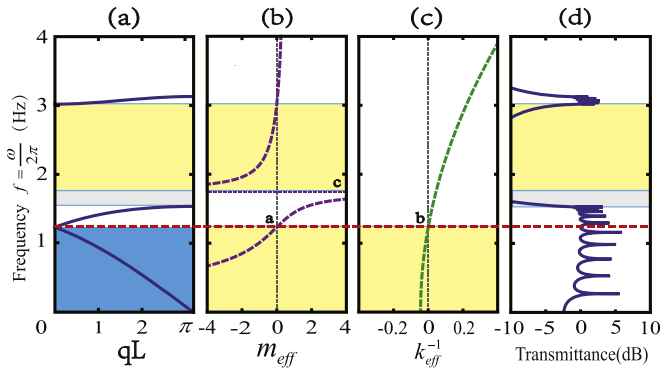

Figure 4. (a) The dispersion relation with a Dirac-like point $f_a = f_b$. (b)–(d) The effective mass, inverse of effective coupling and the transmittance spectrum of the system composed of five units ($N = 5$) with lattice parameters $J = 0.005$ kg m^2, the other parameters are the same as used in figure 2. The red dash line indicates the zero value of m_{eff} and k_{eff}^{-1} at Dirac point.

When the resonant frequencies for translation and rotation are coincident ($f_b = f_c$) (see figure 3), we have $m_{\text{eff}}^{-1} = k_{\text{eff}}^{-1} = 0$. At this condition, the middle band become a flat band and the density of the state is very large. For the system with N units, at the frequency of flat band, there will be N eigenvalues, which means that the system has N vibrational modes. For all of these vibrational modes, we checked that the eigenstates (not shown here) that only the angle displacement of the leverages θ can move but the oscillators m_1 and m_2 stays still, which indicates that the flat band is in accordance with that so-called dark states.

In other words, when a plane wave is incident, the outside balls and inertia balls $m_{1,2}$ can not absorb any energy to move. This is because at this flat-band frequency, both m_{eff}, $k_{\text{eff}} \to \infty$, so that the impedance Z (see the following equation (17)) becomes infinite large. As such, the extremely large impedance mismatch will cause the perfect wave reflection, and at this flat-band the system can not be excited by external incident waves. This is why it is reminiscent of the 'dark state'. These phononic dark states, however, can be excited by brute force-driving the system that evanescently couples with the dark modes. Once the phononic dark states are excited, the energy will be stored within the local vibrations (of leverages in our case), which is not propagating through the system. The transmittance only has a single sharp resonance peak at this resonance frequency, which is very hard to detect from the outside incident wave.

We note that when higher or lower than this flat-band frequency, the system presents respectively the single negative mass regime and single negative coupling regime. The flat band joins together these two single negative metamaterial regimes, so that the two phononic gaps merge into a single wider forbidden gap with the mid-gap dark state negligible. Therefore, tuning the effective negative parameters can cause the total reflection effect in a very wide-spectrum regime to control the wave transmission characteristics, which could finally realize the anti-vibration and the acoustic cloaking [48–50].

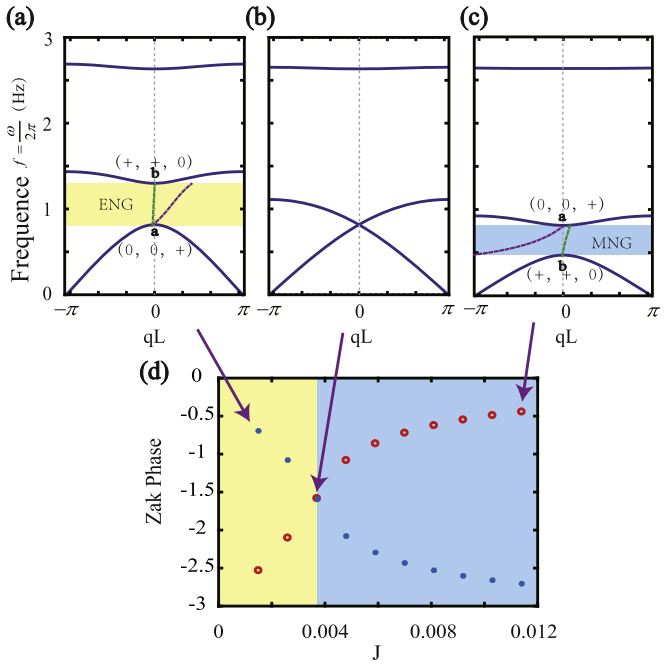

Figure 5. (a)–(c) The dispersion relation of the system by changing the parameters $J, J_a = 0.0015$ kg m^2, $J_b = 0.0038$ kg m^2, $J_c = 0.0114$ kg m^2, the purple dotted line (i) is the effective mass of the system, the green dotted line (ii) is the inverse of effective spring coupling of the system. (d) The curve of the Zak phase for the lower band (the red cross) and the middle band (the blue dotted) with respect to J, $m_1 = 0.25$ kg, $k_2 = 60$ N m^{-1}, other parameters are the same as those in figure 2(a). The yellow areas correspond to ENG and the blue areas correspond to MNG.

3.2. Zero-index at Dirac point

In the continuous limit (i.e. the long wave limit with infinitesimal q), $m_{\text{eff}}\,\partial^2 u/\partial t^2 = -2k_{\text{eff}}\,u(1 - \cos qL)$ can be expanded to be

$$\frac{m_{\text{eff}}}{L}\frac{\partial^2 u}{\partial t^2} = -k_{\text{eff}}Lq^2u = k_{\text{eff}}L\frac{\partial^2 u}{\partial x^2}, \tag{15}$$

due to $q \to i\partial/\partial x$ for harmonic wave solution $u = \hat{u}e^{i(-qx+\omega t)}$. Thus, under this long wave limit, the vibration in 1D phononic metamaterials can be regarded as acoustic/elastic wave, and the discrete lattice can be regarded as a continuous medium. For such a medium, we know that the refractive index is defined as $n = v_s/v_p$ where v_s is the reference sound velocity in air and $v_p = \omega/q = L\sqrt{k_{\text{eff}}/m_{\text{eff}}}$ is the phase velocity in the medium. Thus, the refractive index is

$$n \propto \sqrt{m_{\text{eff}}/k_{\text{eff}}}\,. \tag{16}$$

In addition, the concept of impedance in wave physics is very important, which can govern how a wave propagate in a system. In 1D acoustic metamaterials, the impedance $Z = \rho_{\text{eff}}\,v_p$ with the line density $\rho_{\text{eff}} = m_{\text{eff}}/L$, so that

$$Z = \rho_{\text{eff}}L\sqrt{k_{\text{eff}}/m_{\text{eff}}} = \sqrt{k_{\text{eff}}\,m_{\text{eff}}}\,. \tag{17}$$

Derived from these formulas, if refractive index $n = 0$ (the wave can propagate through the system without any changes), there are two cases to meet it. One is the single zero condition, which means either one of the effective mass m_{eff} and the inverse of effective modulus k_{eff}^{-1} is zero, the other is double zero condition that is both of effective mass and inverse of effective spring coupling equal to zero. If the system is under the single zero condition, we can see that the wave impedance $Z = 0$ or ∞, so that the wave can not pass into the system and propagate in it, due to the strong impedance mismatch. Only under the double zero condition ($m_{\text{eff}} = 0$ and $k_{\text{eff}}^{-1} = 0$), the impedance Z of the system can achieve a finite value so that the impedance of incident wave can match well with the system and the wave will propagate through it, not cause a high reflection at the interface. At the same time, the refractive index n is equal to zero. So the proper necessary condition for zero refractive index is the double zero condition.

For our system, if we want the refractive index $n = 0$, which means the effective mass and the inverse of effective spring coupling are both zero at the same frequency, that is to say the frequency of point a is the same as that of point b ($f_a = f_b$). So we change the lattice parameters of the system and obtain zero refractive index in figure 4(a). A Dirac-like point emerges at the critical point where the lower two pass bands degenerate. In order

to further illustrate it is zero refractive index, we show the distribution of effective mass and the inverse of effective spring coupling in figures 4(b) and (c). Clearly, at the frequency of Dirac-like point, the value of m_{eff} and k_{eff}^{-1} are both zero. In addition, according to the equation (7), using the lattice paraments of figure 4, we calculate the effective mass and the inverse of effective coupling both equal to zero, which meet the double zero condition at the frequency of Dirac-like point.

On the other hand, on the basis of equations (12) and (13), we can obtain the formula of m_1 at Dirac-like point and then substitute it into equation (17), the impedance become

$$Z = \frac{1}{\sqrt{2}R}\sqrt{Jk_2\cos^2\alpha\left(\frac{k_1k_2m_2^2}{(Jk_1/R^2 - k_2m_2)^2} + \cos^2\alpha\right)}. \tag{18}$$

According to the lattice parameters of figure 4, the impedance is calculated and equal to 7.5, which is a finite number indicating that the wave can propagate into the system.

Besides, we also plot the transmittance spectrum of the system at figure 4(d). But the Dirac-like point is not at the peak of the transmittance. The reason is that the boundary condition of the system we use to calculate the dispersion relation and transmittance is different. For the former we adopted periodic system but for the later we use a finite system. So there is a finite shift at the peak of the transmittance. As we increase the number of units, the peak of transmittance converges to that of the Dirac point.

3.3. Band inversion and Zak phases

In the previous section, we obtain the zero refractive index at Dirac-like point through $f_a = f_b$. Then we adjust the lattice parameters to two different setting: $f_a > f_b$,$f_a < f_b$ and find that the second band can flip and become double positive in both setting as shown in figures 5(a)–(c). In figure 5(a), the frequency of point a is higher than the frequency of point b ($f_a > f_b$). The lower frequency band gap at this case is due to the effective negative spring coupling. By further changing the parameters, we obtain figure 5(c). The frequency of point a is lower than the frequency of point b ($f_a < f_b$). It is interesting to find that the lower band gap in this case is caused by negative effective mass. Therefore the two kinds of single negative band gap of figures 5(a) and (c) belong to different topological phases, respectively. The topological phase transition can take place when the system converts from effective elasticity negative (ENG) to effective mass negative (MNG), which is similar to the topological change between ENG (ϵ negative) and MNG (μ negative) in electromagnetism [51–54].

For our system, we first calculate the sign of eigenvectors to judge that whether the band of the system can reverse between the ENG system and the MNG system as shown in figures 5(a)–(c). It is clear that comparing the ENG and MNG systems, the eigenvector signs of the lower band and the middle band exchange with each other at $q = 0$. As such, the two lower bands can reverse as parameters change.

Geometric phases usually characterize the topological properties of Bloch bands. Therefore, we discuss the Zak phase of ENG and MNG systems, which is defined as

$$\theta_n^{\text{Zak}} = \mathrm{i}\int_{-\pi}^{\pi}\left\langle u_{q,n}\left|\frac{\partial}{\partial q}\right|u_{q,n}\right\rangle \mathrm{d}q, \tag{19}$$

where $\langle u_{qn}|\mathrm{i}\partial/\partial q|u_{qn}\rangle$ is the geometric connection. For our system, the unit cell has chiral coupling and is asymmetric, so that it is not easily to define the revolution number of wave vector around origin, and the winding numbers of the system in terms of Zak phases over π will not be quantized [55]. But, according to the curve of Zak phases for the lower band (the red cross) and the middle band (the blue dotted) as a function of J (figure 5(d)), we can still observe that as the parameter J changes, Zak phases of two bands also cross with each other, and the property of the system changes from coupling-negative to mass-negative. Meanwhile, the lower band and the middle band close (figure 5(b)) and reopen again, so that band inversion occurs. We should point out that when the parameter J tends to zero (infinity), the Zak phase of the lower band and the middle band tend to $-\pi$ (0) and 0 ($-\pi$). Similar phase transitions can be also observed by tuning other system's parameters.

3.4. Topological interface states

Topological interface states can exist in the interface between two simple lattices of distinct topological phases. In order to verify the topological phase transition between ENG and MNG phononic metamaterials, we construct a two-segment structure as shown in figure 6(a) to manifest topological interface states in the lower band gap. The left five units are constructed as the system with effective negative spring coupling (ENG) in certain frequency range and the right five units are constructed as the system with effective negative mass (MNG) in the same frequency range.

In order to get a more intuitive view of the interface state, we plot the transmittance of the system in figure 6(b). The upper part of the figure is the transmittance of the system and the lower part indicates the positions of eigenvalues. The eigenvalue matches well with the frequency of the resonance peaks. Clearly, there is

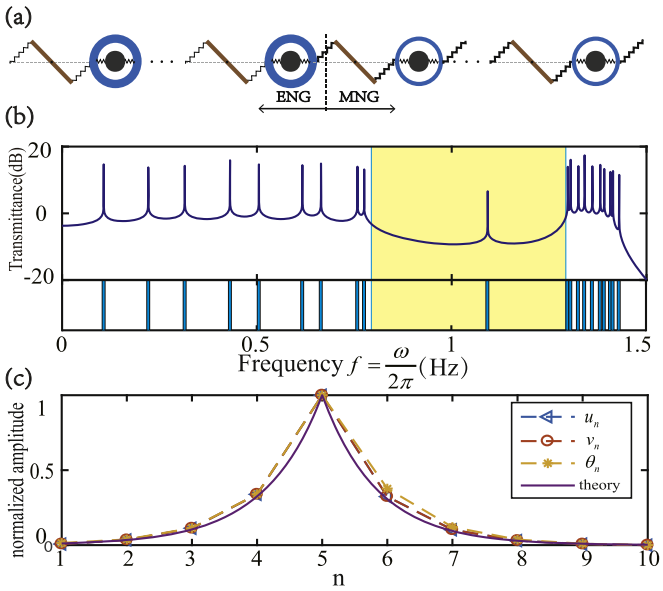

Figure 6. (a) The schematic spring-mass model of a 1D system to achieve the topological interface state with $N = 10$. The left lattice is effective elasticity negative (ENG, $m_1 = 0.5$ kg, $k_2 = 20$ N m^{-1}, $J = 0.0015$ kg m^2) and the right lattice is effective mass negative (MNG, $m_1 = 0.25$ kg, $k_2 = 60$ N m^{-1}, $J = 0.0114$ kg m^2) in the same frequency range mentioned above. The last spring is added to change the edge-mode. (b) The transmittance spectrum and eigenvalue of the system composed of ten units ($N = 10$). (c) The spatial profile of the eigenmodes of the interface state for the finite structure ($N = 10$). The purple solid line is theoretical results of u_n. The blue triangle, orange circle and yellow star dashed line are respectively the eigenmode of u_n, v_n and θ_n. Other parameters of the system are the same as those in figure 2.

a resonance peak within the gap, so-called mid-gap state. The spatial profile of the eigenmodes at the resonance frequency is shown in figure 6(c). We can see that the resonant states at the five units and the amplitudes exponential decay on both sides of the interface between the ENG and MNG lattices. The resonance peak is reminiscent of the topological Jackiw–Rebbi interface state in the quantum field theory [56].

To understand the emergence of the interface state, we take the long wave limit as mentioned above. The 1D single lattice wave can be regarded as elastic wave and the wave number $q = \omega\sqrt{m_{\text{eff}}/k_{\text{eff}}}/L$. For a single negative system, $\sqrt{m_{\text{eff}}/k_{\text{eff}}}$ is an imaginary number. Thus, we can let $q \equiv -\mathrm{i}\kappa$ [57], where

$$\kappa = \omega\sqrt{|m_{\text{eff}}/k_{\text{eff}}|}/L. \tag{20}$$

At the middle interface ($x = 0$), the boundary condition is that the force and the displacement must be continuous, so that

$$\begin{aligned} F_L &= F_0 \mathrm{e}^{\kappa_L x + \mathrm{i}\omega t},\ F_R = F_0 \mathrm{e}^{-\kappa_R x + \mathrm{i}\omega t}; \\ u_L &= u_0 \mathrm{e}^{\kappa_L x + \mathrm{i}\omega t},\ u_R = u_0 \mathrm{e}^{-\kappa_R x + \mathrm{i}\omega t}. \end{aligned} \tag{21}$$

According to the continuous version of Newton's equation of motion, $\rho_{\text{eff}}\,\mathrm{d}^2u/\mathrm{d}t^2 = -\partial F/\partial x$ (substituting $F = -k_{\text{eff}}L\partial u/\partial x$ into equation (15)), we obtain that: $\omega^2 m_{\text{eff},L(R)}u_0/L = \pm\kappa_{L(R)}F_0$ should be hold on two sides of the interface. Therefore,

$$\frac{m_{\text{eff},L}}{\kappa_L} = -\frac{m_{\text{eff},R}}{\kappa_R} \Longrightarrow m_{\text{eff},L}k_{\text{eff},L} = m_{\text{eff},R}k_{\text{eff},R}. \tag{22}$$

Clearly, this condition indicates that the resonance peak meets the condition of impedance matching.

$$Z_{\text{ENG}} = Z_{\text{MNG}}. \tag{23}$$

The closer the impedance of the two media is, the easier the wave will pass through the interface and cause a resonance peak. So, in our system, the wave impedance of the left lattice (ENG) and right lattice (MNG) are equal to each other at the resonance frequency.

For the system in figure 6(a), the interface is at $n = 5$. Using the lattice parameters of the system in figure 6, we can calculate out the resonance frequency $f_{\text{in}} = \omega/(2\pi)$ satisfying equation (22) as $f_{\text{in}} = 1.09$ Hz. The penetration length of the interfacial evanescent wave is characterized by $1/\kappa$ from equation (20). The calculations from the continuous wave equation with impedance analysis agree well with the observation from the discretized lattice in figure 6. At f_{in}, the left lattice and right lattice both have single negative property in the lower band gap, where their impedances match with each other to support the interface state.

4. Conclusion

In summary, we have shown that, the system we studied exhibits different effective properties, such as double positive, single negative or double negative parameters (mass and coupling), depending on the incident frequency. By calculating the transmission characteristics, we have observed that there is a low transmittance in the band gap which can be used to design vibration-resistance materials. At the frequency where the effective mass and coupling are both infinite, a flat band emerges that will induce an extremely high density of states and the system possesses dark states. We have also achieved zero refraction index by adjusting the parameters for forming a Dirac-like point, where both effective mass $m_{\text{eff}} = 0$ and the inverse of effective spring coupling $k_{\text{eff}}^{-1} = 0$ such that the wave impedance is finite, which have wide application prospects on wave manipulations. Besides, the phenomenon of topological phase transition between negative mass and negative coupling has been studied in the low frequency band gap. Finally, we have analyzed the interface state arising from distinct topological phase between ENG and MNG. These properties will deepen our understanding in both physics and application on the emerging concept of one-dimensional topological phononic metamaterials. The system we used could be realized in experiment by the magnetic levitation guide or a thin string [44] to resist the influence of gravity.

Acknowledgments

This work is supported by the National Natural Science Foundation of China (No. 11775159, 11935010), the Shanghai Science and Technology Commitee (No. 18ZR1442800, No. 18JC1410900), the Opening Project of Shanghai Key Laboratory of Special Artificial Microstructure Materials and Technology.

ORCID iDs

Jie Ren https://orcid.org/0000-0003-2806-7226

References

[1] Veselago V G and Lebedev P N 1968 *Sov. Phys.—Usp.* **10** 509
[2] Pendry J B, Holden A J, Stewart W J and Youngs I 1996 *Phys. Rev. Lett.* **76** 4773
[3] Pendry J B, Holden A J, Robbins D J and Stewart W J 1999 *IEEE Trans. Microw. Theory Tech.* **47** 2075
[4] Smith D R, Padilla W J, Vier D C, Nematnasser S C and Schultz S 2000 *Phys. Rev. Lett.* **84** 4184
[5] Smith D R and Kroll N 2000 *Phys. Rev. Lett.* **85** 2933
[6] Shelby R A, Smith D R and Schultz S 2001 *Science* **292** 77
[7] Liu Z Y, Zhang X X, Mao Y W, Zhu Y Y, Yang Z Y, Chan C T and Sheng P 2000 *Science* **289** 1734
[8] Li J and Chan C T 2004 *Phys. Rev.* E **70** 055602
[9] Ding Y Q, Liu Z Y, Qiu C Y and Shi J 2007 *Phys. Rev. Lett.* **99** 093904
[10] Wu Y, Lai Y and Zhang Z Q 2011 *Phys. Rev. Lett.* **107** 105506
[11] Bongard F, Lissek H and Mosig J R 2010 *Phys. Rev.* B **82** 094306
[12] Finocchio G, Casablanca O, Ricciardi G, Alibrandi U, Garesci F, Chiappini M and Azzerboni B 2014 *Appl. Phys. Lett.* **104** 509
[13] Fang N X, Xi D J, Xu J Y, Ambati M, Srituravanich W, Sun C and Zhang X 2006 *Nat. Mater.* **5** 452
[14] Lee S H, Park C M, Yong M S, Zhi G W and Kim C K 2008 *J. Phys.: Condens. Matter* **21** 175704
[15] Yang Z Y, Mei J, Yang M, Chan N H and Sheng P 2008 *Phys. Rev. Lett.* **101** 204301
[16] Lee S H, Park C M, Seo Y M, Wang Z G and Kim C K 2010 *Phys. Rev. Lett.* **104** 054301
[17] Liang Z X, Feng T H, Lok S, Liu F, Ng K B, Chan C H, Wang J J, Han S, Lee S and Li J 2013 *Sci. Rep.* **3** 1614
[18] Xie Y B, Popa B I, Zigoneanu L and Cummer S A 2013 *Phys. Rev. Lett.* **110** 175501
[19] Torrent D and Sanchezdehesa J 2008 *New J. Phys.* **10** 023004
[20] Kaina N, Lemoult F, Fink M and Lerosey G 2015 *Nature* **525** 77
[21] Liu X N and Hu G K 2016 *Strojniski Vestn.* **62** 403
[22] Lee S H and Wright O B 2016 *Phys. Rev.* B **93** 024302
[23] Milton G W and Willis J R 2007 *Proc. R. Soc.* A **463** 855
[24] Yao S S, Zhou X M and Hu G K 2008 *New J. Phys.* **10** 043020
[25] Liu X N, Hu G K, Sun C T and Huang G L 2011 *J. Sound Vib.* **330** 2536
[26] Liu X N, Hu G K, Huang G L and Sun C T 2011 *Appl. Phys. Lett.* **98** 251907
[27] Huang H H and Sun C T 2011 *J. Mech. Phys. Solids* **59** 2070
[28] Zhu R, Liu X, Hu G, Sun C and Huang G 2014 *J. Sound Vib.* **333** 2759
[29] Zhu R, Liu X N, Hu G K, Sun C T and Huang G L 2014 *Nat. Commun.* **5** 5510
[30] Foehr A, Bilal O R, Huber S D and Daraio C 2018 *Phys. Rev. Lett.* **120** 205501
[31] Engheta N 2013 *Science* **340** 286
[32] Liu R P, Cheng Q, Hand T H, Mock J J, Cui T J, Cummer S A and Smith D R 2008 *Phys. Rev. Lett.* **100** 023903
[33] Edwards B, Alu A, Young M E, Silveirinha M and Engheta N 2008 *Phys. Rev. Lett.* **100** 033903
[34] Zheng L Y, Wu Y, Ni X, Chen Z G, Lu M H and Chen Y F 2014 *Appl. Phys. Lett.* **104** 1619047
[35] Dubois M, Shi C Z, Zhu X F, Wang Y and Zhang X 2017 *Nat. Commun.* **8** 14871
[36] Liu F M, Huang X Q and Chan C T 2012 *Appl. Phys. Lett.* **100** 071911

[37] Hyun J, Choi W, Wang S, Park C and Kim M 2018 *Sci. Rep.* **8** 7288 https://www.dropbox.com/s/8zo54uc1mjjb0r2/000037.JPG?dl=0
[38] Zhu X F 2013 *Phys. Lett.* A **377** 1784
[39] Zhang L F, Ren J, Wang J S and Li B W 2011 *J. Phys.: Condens. Matter* **23** 305402
[40] Zhang L F, Ren J, Wang J S and Li B W 2010 *Phys. Rev. Lett.* **105** 225901
[41] Li N B, Ren J, Wang L, Zhang G, Hänggi P and Li B W 2012 *Rev. Mod. Phys.* **84** 1045
[42] Zhao D G, Xiao M, Ling C W, Chan C T and Fung K H 2018 *Phys. Rev.* B **98** 014110
[43] Liu Y Z, Lian C S, Li Y, Xu Y and Duan W H 2017 *Phys. Rev. Lett.* **119** 255901
[44] Salerno G, Berardo A, Ozawa T, Price H M, Taxis L, Pugno N M and Carusotto I 2017 *New J. Phys.* **19** 055001
[45] Xiao M, Zhang Z Q and Chan C T 2014 *Phys. Rev.* X **4** 021017
[46] Xiao M, Ma G C, Yang Z, Sheng P, Zhang Z Q and Chan C T 2015 *Nat. Phys.* **11** 240
[47] Wang P, Lu L and Bertoldi K 2015 *Phys. Rev. Lett.* **115** 104302
[48] Chen H Y and Chan C T 2007 *Appl. Phys. Lett.* **91** 183518
[49] Cai L W and Sachezdehesa J 2007 *New J. Phys.* **9** 450
[50] Cummer S A, Popa B I, Schurig D, Smith D R, Pendry J, Rahm M and Starr A 2008 *Phys. Rev. Lett.* **100** 024301
[51] Tan W, Sun Y, Chen H and Shen S Q 2014 *Sci. Rep.* **4** 3842
[52] Shi X, Xue C H, Jiang H T and Chen H 2016 *Opt. Express* **24** 18580
[53] Guo Z W, Jiang H T, Long Y, Yu K, Ren J, Xue C H and Chen H 2017 *Sci. Rep.* **7** 7742
[54] Long Y, Ren J, Jiang H T, Sun Y and Chen H 2017 *Acta Phys. Sin.* **66** 227803
[55] Atala M, Aidelsburger M, Barreiro J T, Abanin D A, Kitagawa T, Demler E and Bloch I 2013 *Nat. Phys.* **9** 795
[56] Shen S Q 2012 *Topological Insulators* (Berlin: Springer)
[57] Lee M H, Jung M K and Lee S H 2012 *J. Korean Phys. Soc.* **60** 31